Available online at www.sciencedirect.com

ScienceDirect

Ceramics International 40 (2014) 31–38

CERAMICS INTERNATIONAL

www.elsevier.com/locate/ceramint

Mechanical alloying, sintering and characterization of Al_2O_3–20 wt%–Cu nanocomposite

Mahmoud F. Zawrah[a,*], Raghieba A. Essawy[b], Hamdia A. Zayed[c], Amira H. Abdel Fattah[b], Mohammed A. Taha[b]

[a]*Ceramics Department, National Research Center, Dokki, Cairo, Egypt*
[b]*Solid State Physics Department, National Research Center, Dokki, Cairo, Egypt*
[c]*Physics Department, Faculty of Girls, Ain-Shams University, Egypt*

Received 7 May 2013; received in revised form 24 May 2013; accepted 27 May 2013
Available online 6 June 2013

Abstract

Alumina-based matrix nanocomposite powder reinforced with 20 wt%-Cu particles was fabricated by mechanical alloying. The starting powders mixture was milled in a planetary ball mill up to 20 h. The effect of milling time on the properties of obtained powders was studied. X-ray diffraction analysis (XRD) and transmission electron microscopy (TEM) were used to investigate phase composition, crystallite size and morphology of the milled powders. To study the sinterability, the milled nanocomposite powders were cold pressed at 10 MPa and sintered in argon atmosphere at different firing temperatures, i.e. 1100, 1250, 1400, 1500 and 1550 °C, for 1 h. Physical properties, namely, bulk density and apparent porosity of sintered bodies were determined by the Archimedes method. Phase identification and microstructure of the sintered composites were investigated by using scanning electron microscopy (SEM) as well as energy dispersive spectrometry (EDAX). Microhardness and fracture toughness of sintered composite were also examined using Vickers indentor. The results revealed that a uniform distribution of Cu reinforcement in Al_2O_3 matrix, coating the particles, was successfully obtained after milling the powders. Also, there was no sign of phase changes during the milling. The crystallite size decreased at prolonged milling time while the internal strain increased. The maximum relative density was obtained after sintering at 1550 °C. The hardness of the sintered composite improved while the fracture toughness slightly decreased with the prolongation of milling time.

Keywords: A. Sintering; C. Mechanical properties; Mechanical alloying; Al_2O_3-based composites

1. Introduction

Al_2O_3 is a very useful industrial material and the most widely used ceramic. It possesses favorable mechanical properties such as: high hardness, high compressive strength, good chemical and thermal stabilities and high elastic modulus [1]. However, its application as a structural material has been limited due to its low fracture toughness and low fracture strength. Because of easy propagation of cracks in ceramics; thus, they fail unexpectedly in service. Several authors have reported that the incorporation of some amounts of small-sized metal in ceramic matrix could result in an improvement of its fracture toughness. For example, they have reported the production of alumina based composites having different amount of metals by diverse methods, e.g. Al_2O_3/Cu [2], Al_2O_3/Al [3], Al_2O_3/Ni [4]. Improved fracture toughness have been achieved for such composites.

In recent years, Al_2O_3/Cu composite has been attracting researcher's interest since it can provide many advantageous characteristics, such as high thermal and electrical conductivities, high strength and excellent resistance to high temperature annealing [5]. In particular, interesting studies have been made using mechanical alloying for fabrication of Al_2O_3-based ceramics containing copper; where the effect of copper particles dispersed in the ceramic was analyzed. The reinforcement models indicated that the size of metallic inclusion is very important to adhere metallic particles to ceramic matrix. Moreover, help in homogeneous distribution of metallic particles in the matrix in order to obtain a composite material with good properties [6,7].

Mechanical alloying (MA) is a simple and useful technique for attaining a homogeneous distribution of inert fine particles within

*Corresponding author. Fax: +20233370931.
E-mail address: mzawrah@hotmail.com (M.F. Zawrah).

0272-8842/$ - see front matter © 2013 Elsevier Ltd and Techna Group S.r.l. All rights reserved.
http://dx.doi.org/10.1016/j.ceramint.2013.05.099

a fine grained matrix [8]. The MA is an unique process in which a solid state reaction takes place between the fresh powder surfaces of the reactant materials at room temperature. Consequently, it can be used to produce alloys and compounds which are difficult or impossible to be obtained by the conventional melting and casting techniques [9]. Mechanical alloying (MA) has been found as a useful method for improving the reinforcement particle distribution not only in microcomposites [10,11] but also in nanocomposites [12–14]. Generally, MA is performed in three steps [15]. Firstly, powders suffer impacts among them and balls with little fracture and plastic deformation. In the second step, plastic deformation and cold welding process predominate. Finally, powders harden and then fracture due to the continuous increase of plastic deformation giving rise to a new and smaller surfaces. In this step, there is a balance between cold welding and fracture frequency. Therefore, it can be said that the "steady state condition" has been reached. Further processing time will not cause significant effect on the particle size, shape and morphology [16].

The present work focuses on studying the effect of milling time on the morphology and crystallite sizes of Al_2O_3–20 wt%–Cu composite. Moreover, the effects of milling time and sintering temperature on its sinterablity and mechanical properties were addressed.

2. Materials and experimental procedures

Mixture of Al_2O_3 and Cu powders having 98.2% and 99.9% purity as well as ≥1.4 and 10 μm average particle sizes, respectively, was used as starting materials to prepare Al_2O_3–20 wt%–Cu nanocomposite. Stearic acid was also used as process controlling agent to prevent the agglomeration of powders mixture during milling. The powders mixture was milled in a planetary ball mill, type SFM-1Desk-Top, up to 20 h at rotating speed 500 rpm and ball-to-powder weight ratio of 10:1. Al_2O_3 and ZrO_2 balls having diameters 6–20 mm were utilized as milling media. The proposed composite constituents (Al_2O_3–20 wt%–Cu) were selected according to our unpublished data and the data published in the literatures which indicated that the appropriate percent of Cu to give compromised mechanical properties is 20%. Phase identification of the milled powders was conducted by X-ray diffraction analysis (XRD) using "Philips PW 1373" X ray powder diffractometer with CuK–Ni filtered radiation. XRD patterns were recorded in the 2θ range between 22 and 80 and the diffraction patterns were recorded automatically with a scanning rate 2 deg/min.

The lattice parameter "a" of the obtained phases was calculated for the principle (*hkl*) planes (104, 103, 012 and 116) according to the following equation [17]:

$$\frac{1}{d^2} = \frac{h^2 + k^2 + l^2}{a^2}$$

The crystallite size (D) was determined from the broadening (β) of the same four diffraction lines (104, 103, 012 and 116) using the Scherrer equation as the following [18,20]:

$$D = \frac{0.9\,\lambda}{\beta \cos\,\theta}$$

The lattice strain (ε) was calculated for the same diffraction lines from the following equation [19,20]:

$$\varepsilon = \frac{\beta}{4\tan\,\theta}$$

where λ=1.54059 °A (Cu–Ni radiation), β is the full width at half maximum and θ is the angle in radians.

A transmission electron microscopy (TEM type JEOL JEM-1230 operating at 120 kV attached to a CCD camera) was employed to investigate the morphology and grain size of the obtained powders after different milling time.

The milled composite powders were cold-compacted into small compacts of desired sizes at room temperature. Samples of 10 mm diameter and 4 mm height were compacted using a hardened steel die set. A hydraulic press was used for pressing the specimen at 10 MPa. The compacted samples were sintered at different temperatures i.e. 1100, 1250, 1400, 1500 and 1550 °C in argon atmosphere for 1 h and heating rate 8 °C/min.

Relative density and apparent porosity of the sintered parts were determined by using 'Archimedes' principle. The theoretical densities of compacts was calculated from the simple rule of mixtures taking the fully dense values for Al_2O_3 and Cu were 3.95 and 8.96 g/cm^3, respectively. The relative density was calculated using the measured bulk density and calculated theoretical density. Average values of three reading for bulk density and porosity were reported. The microstructure of sintered samples was characterized by scanning electron microscopy (SEM), type "Philips XL30".

Microhardness (Vickers hardness) of the sintered specimens was determined according to ASTM standards E 284-99, 1327-03 and C 1326-03, using a UNITED TRU-BLUE UNIVERSAL hardness tester with a load of 98 N (10 kg). Load for 10 s was applied during measuring of the hardness [21–23]. The hardness values of the investigated materials were measured as average of five readings along the cross section surface of the specimens.

The fracture toughness, K_{IC}, of sintered samples was determined from the indentation fracture (IF) using Vickers hardness test [24,25]. The fracture toughness, K_{IC}, of bulk samples was calculated using the following equation:

$$K_{IC} = 0.016\,H_V\,X\,\frac{a^2}{C^{3/2}}$$

where a is half length of diagonal of the indent and c is crack length from the center of the indentation to the crack end. The fracture toughness values of the investigated materials were measured as the average of five readings along the cross section surface for each sample.

3. Results and discussion

3.1. Characterization of the prepared powders

3.1.1. Phase composition of the prepared powders

Fig. 1 shows XRD patterns of Al_2O_3–20 wt%–Cu composites produced after different milling times. It appears that only two phases of Al_2O_3 and Cu were found in the pattern of the milled powders following to the card numbers (88-0826 and

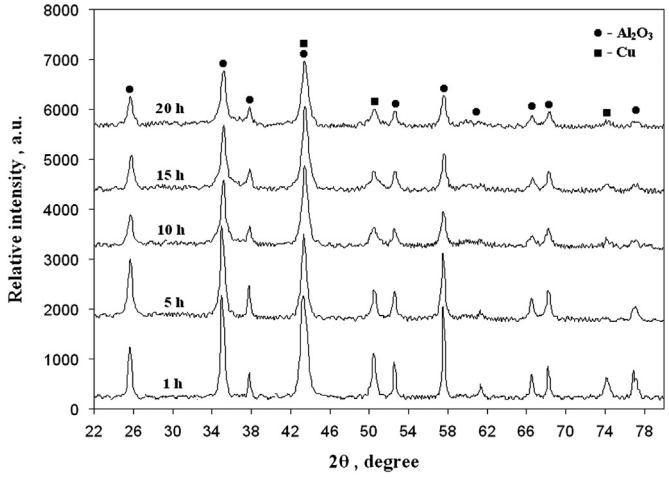

Fig. 1. XRD of Al_2O_3–20 wt%–Cu powder composites produced after different milling times.

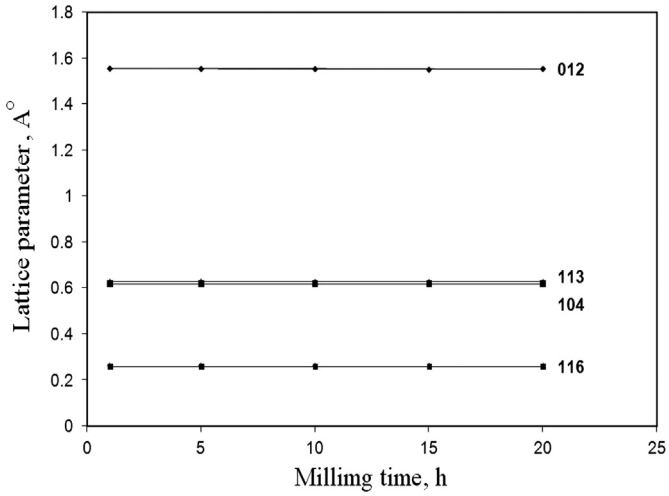

Fig. 2. Lattice parameter vs. milling time of Al_2O_3–20 wt%–Cu powder mixtures.

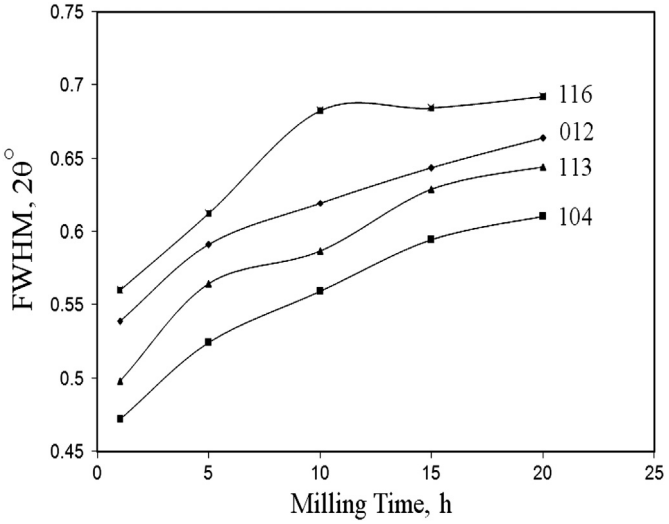

Fig. 3. Full width at half maximum (FWHM) of Al_2O_3–20 wt%–Cu vs. milling time.

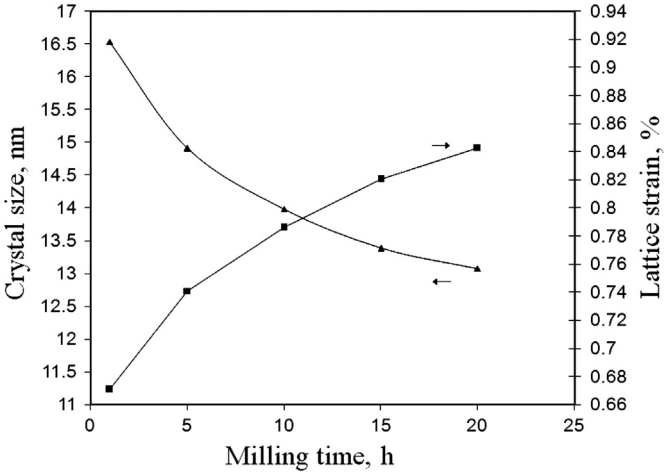

Fig. 4. Crystallite size and lattice strain of Al_2O_3–20 wt%–Cu measured at different milling time.

85-1326) [26,27]. It is also found that with increasing of milling time, the diffraction peaks of Al_2O_3 and Cu became broader and their intensities became weaker. These changes reveal a reduced grain size and an elevated strain energy stored inside particles because of the severe plastic deformation introduced during ball.

Fig. 2 exhibits the relationship between lattice parameter and milling time. During the milling of Al_2O_3–20 wt%–Cu composite, lattice parameter remains constant with increasing milling time due to neither solid solution formation between Al_2O_3 and Cu nor Cu oxidation during milling.

Fig. 3 depicts full width at half maximum (FWHM) of milled powders. A progress in line broadening with increasing of milling time is detected. This is due to severe lattice distortion and grain size refinement [28,29].

Crystallite size and lattice strain of Al_2O_3–20 wt%–Cu nanocomposite vs. milling time are shown in Fig. 4. It is indicated that the crystallite size (D) decreased with increasing of milling time (t) according to the equation $D = Kt^{-2/3}$, where K is a constant [15,30]. From the figure, it is indicated that the crystallite size of the powders decreases rapidly during initial milling up to 10 h and then more slowly as the milling time increases [31,32]. The lattice strain increases with increasing of milling time due to distortion effect caused by dislocation in the lattice [15,33]. The lattice strain curve has a maximum value at 20 h which is ascribed to the crystallite size reduction.

3.1.2. Morphology of the prepared powders

Transmission electron microscopy was used to gain better insight into the microstructure of the composite powder. During high energy milling, the powder particles change their morphology and size as a consequence of repeated deformation, fracturing and welding processes. In the first stage of milling, the ductile particles undergo deformation while the brittle particles undergo fragmentation. Then, when ductile particles start to weld, the brittle particles come between two or

more ductile particles at the instant of ball collision. As a result, fragmented reinforcement particles reside at the interfacial boundaries of the welded metal particles, and the result is the formation of real composite particles [19].

Fig. 5 exhibits TEM images of Al_2O_3–20 wt%–Cu composite powders. At the early stage of milling i.e. 1 and 5 h, the Cu particles undergo deformation and appear as inhomogenously distributed between Al_2O_3 particles with size decreasing. With increasing of milling time up to 10 h, the Cu particles started to coat Al_2O_3 particles and the particles size decreased but still inhomogeneous in shape (Fig. 5c). At the final stage of milling (15 and 20 h), Al_2O_3 is completely coated by Cu particles and the particle size has decreased after 15 h milling. Slight decrease in the size is detected after milling for 20 h.

The effect of milling time on the particle size of different composite powders has been studied. The average particle size of the milled powders was obtained from TEM observation

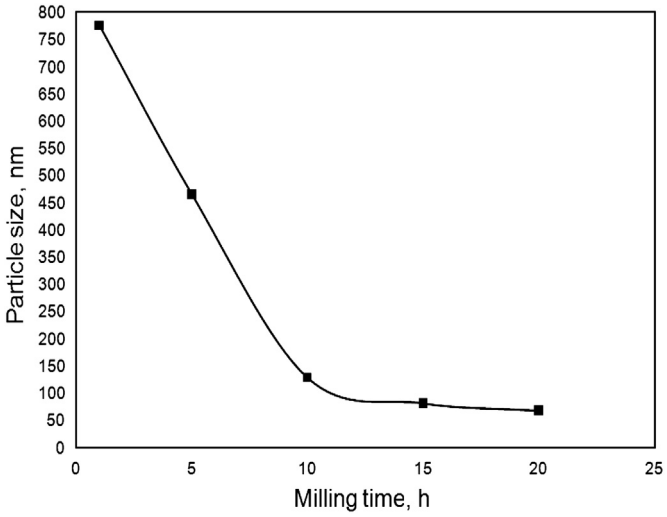

Fig. 6. Particle size of Al_2O_3–20 wt%–Cu milled for different milling time.

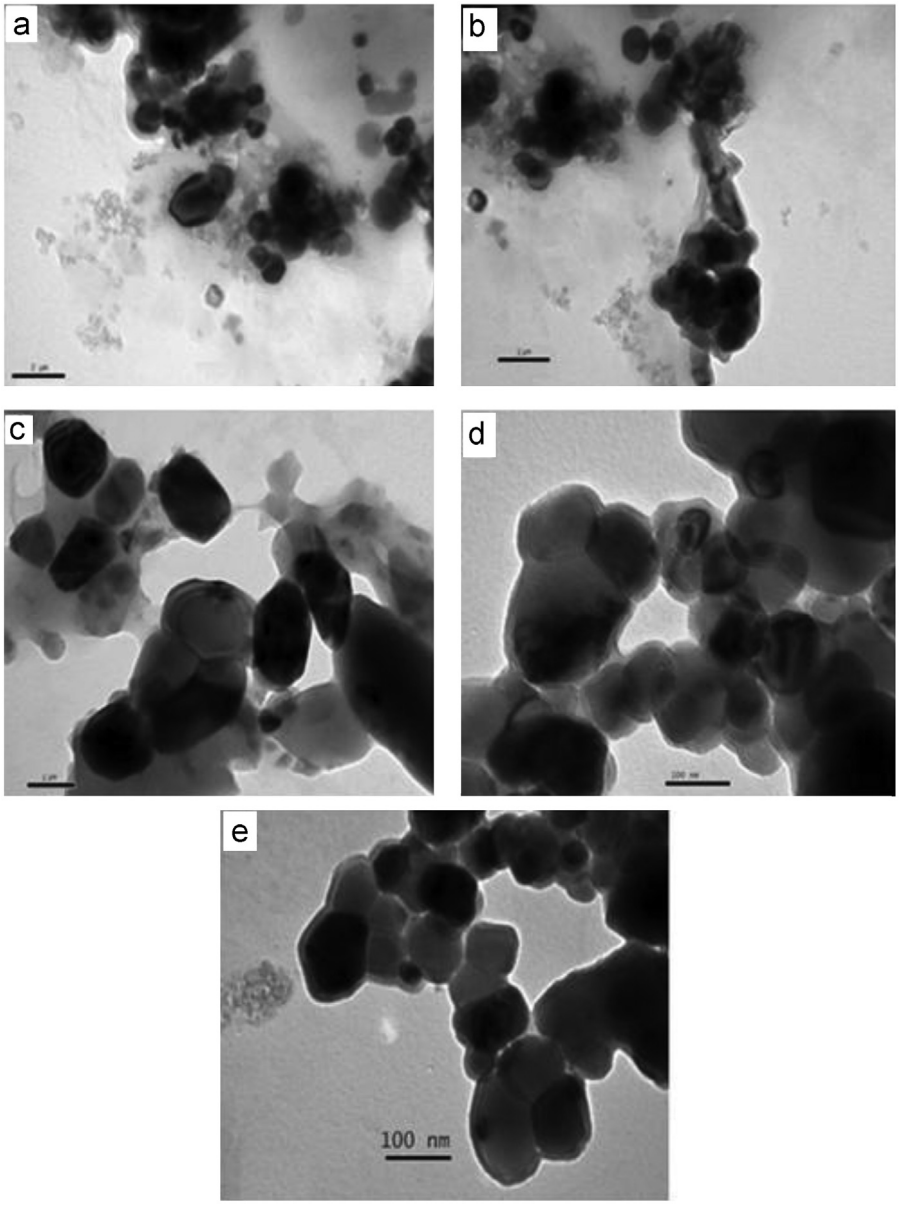

Fig. 5. TEM photomicrographs of Al_2O_3–20 wt%–Cu particles milled for different milling time, (a) 1 h, (b) 5 h, (c) 10 h, (d) 15 h, and (e) 20 h.

and presented in Fig. 6. It is indicated that the particle size decreases with the increase of milling time.

3.2. Sinterability of the prepared nanocomposites

3.2.1. Relative density and apparent porosity

The effect of milling time of starting powders on relative density and apparent porosity of the sintered samples prepared at different temperatures i.e. 1100, 1250, 1400, 1500 and 1550 °C for 1 h in argon is shown in Fig. 7. Firstly, the theoretical density of Al_2O_3–20 wt%–Cu composite was calculated by the mixture rule and its value was 4.823 g/cm^3. The relative density of the sintered samples increased with increasing of both milling time and sintering temperature. On the other hand, apparent porosity decreased with increasing of both milling time and sintering temperature [34–38]. With increasing milling time, the particle size of starting power decreases leading to the increase of compactness and consequently sinterability of the composites. Increasing sintering temperature enhances the diffusion of grains and solid–solid as well as solid–liquid interactions leading to increase of the sinterability.

3.2.2. Microstructure of the sintered composites

Microstructure of the sintered samples at 1550 °C for 1 h in argon atmosphere, in relationship with milling time of the starting materials, is shown in Fig. 8. Microstructure with fine Al_2O_3 grains is observed. The gray phase corresponds to Al_2O_3 matrix, while as the lighter phase corresponds to Cu phase which is localized on the grain boundaries. Also, some

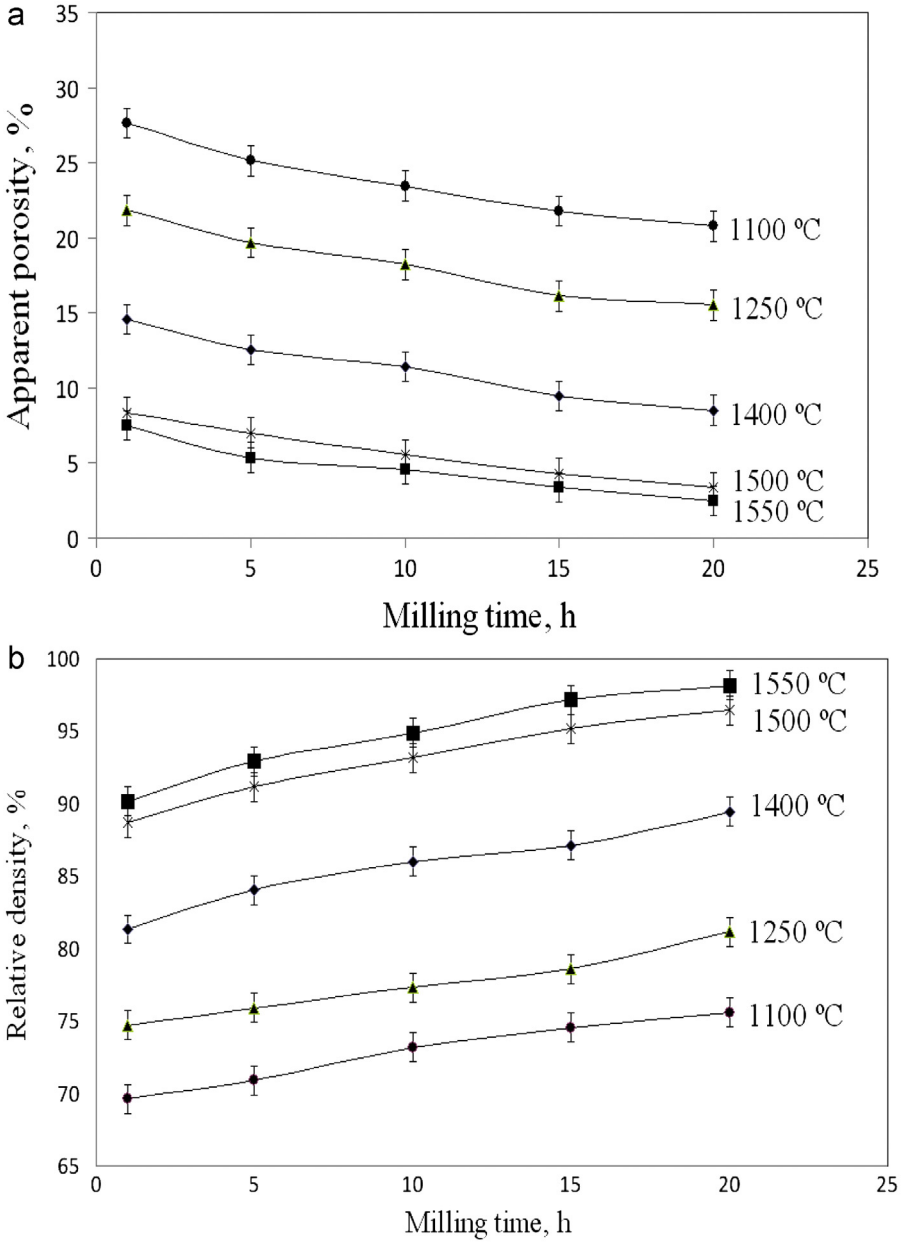

Fig. 7. Effect of milling time and sintering temperature on (a) relative density and (b) apparent porosity of sintered composites.

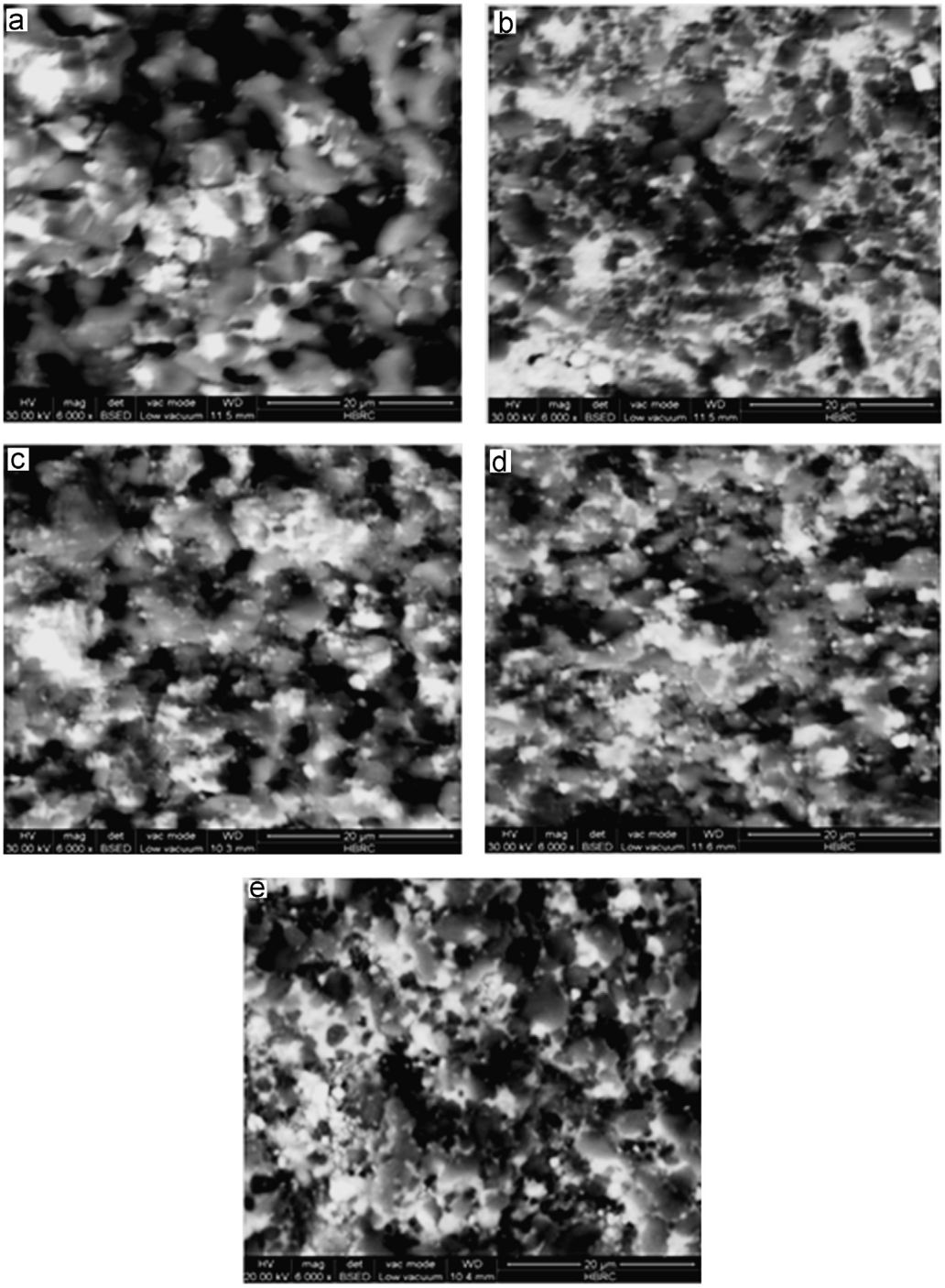

Fig. 8. SEM microphotographs of the sintered Al_2O_3–20 wt%–Cu for 1 h at 1550 °C prepared from powders milled at different milling time (a) 1 h, (b) 5 h, (c) 10 h, (d) 15 h, and (e) 20 h.

pores are observed and localized in intergranular zones. Increasing milling time caused a uniform distribution of the reinforced particles, reduction in particles size (even to nanometer), and disappearing of particle agglomeration. But the possibility of forming agglomerates during milling due to particle segregation caused by variation in powder densities and nano-sized particles should be taken in consideration. As clearly observed, Cu is well dispersed in the alumina matrix wetting their particles and forming a good homogenous and dense microstructure. Due to the relatively higher sintering temperature, some alumina nanoparticles formed alumina clusters inside the copper coat. The microstructure of sintered sample prepared from powder milled for 1 h (Fig. 8a) exhibits higher alumina grain size as compared with those prepared after milling up to 20 h (Fig. 8b–e). EDX analysis of sintered Al_2O_3–20 wt%–Cu composite for 1 h at 1550 °C and prepared after 20 h milling time is shown in Fig. 9. The presence of trace zirconium oxide came from contamination during ball milling through the milling media.

3.2.3. Microhardness and fracture toughness of sintered composite

The effect of milling time of starting powders on microhardness and fracture toughness of Al_2O_3–20 wt%–Cu composite sintered for 1 h at 1550 °C in argon, is shown in Fig. 10. Generally, microhardness of composites increased with increasing of milling time due to the grain refinement, while as the fracture toughness reduced slightly with increasing of milling time. This is probably due to the trace impurities such as Fe_2O_3, SiO_2 and CaO present the starting alumina powder. Similar results were reported in the Ref. [39].

Generally, increasing toughness in ceramic composites can be explained by any one or more of the four mechanisms namely crack bowing, crack deflection, crack bridging and stress-induced microcracking [40]. The toughening mechanism believed to be particularly effective in ceramic/metal composites is the plastic stretching of metallic inclusions which bridges and deflects the growing of cracks [41]. From microstructural observation of the cracks introduced by the Vickers indentation on the surface of the composites, the presence of crack deflection was detected, as shown in Fig. 11. Thus, in this composite system the crack deflection resulting from the ductile behavior of Cu particles and crack deflection are thought to be the main reasons for the toughness enhancement.

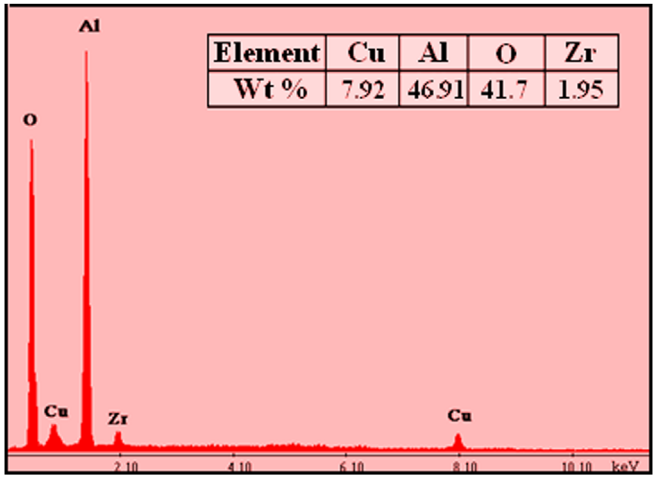

Fig. 9. EDX spectra of Al_2O_3–20 wt%–Cu composite sintered for 1 h at 1550 °C prepared from powders milled at 20 h.

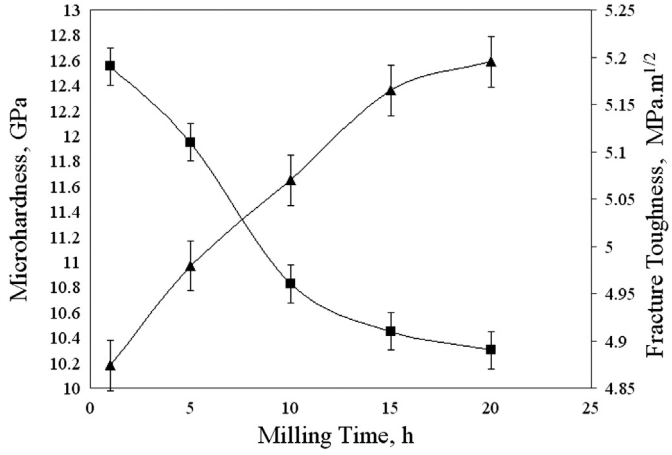

Fig. 10. Microhardness of sintered Al_2O_3–20 wt%–Cu compacts vs. milling time.

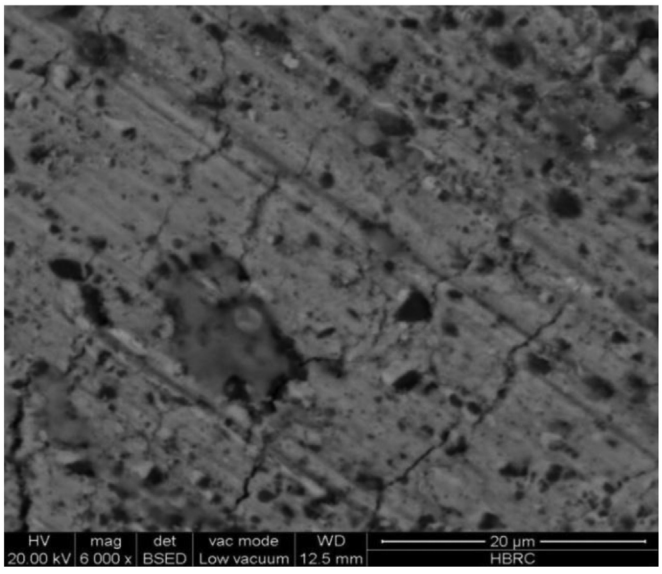

Fig. 11. SEM microphotograph showing crack propagation on the surface of Al_2O_3–20 wt%–Cu composite sintered for 1 h at 1550 °C prepared from powder milled for 20 h.

4. Conclusion

The following remarks were concluded:

- Al_2O_3–20 wt%–Cu nanocomposites have been fabricated by the mechanical alloying technique in planetary ball mill after different milling time up to 20 h. After milling, grain refinement took place and fine Cu particles were regularly distributed in the Al_2O_3 matrix. After 20 h milling, the size of Al_2O_3–20 wt%–Cu nanocomposite particles was 68 nm. A uniform distribution of nanosized Cu reinforcement throughout the Al_2O_3 matrix, coating the particles, was successfully obtained.
- The crystallite size has been decreased while the lattice strain was found to increase with increasing of milling time due to distortion effect caused by dislocation in the lattice.
- The relative density of the sintered bodies was increased with increasing both milling time of starting powders and sintering temperature. On the other hand, apparent porosity was decreased.
- The microhardness of the sintered composites was improved while the fracture toughness was reduced with increasing of milling time for starting powder.

References

[1] J.K. Wessel, The Handbook of Advanced Materials, John Wiley & Sons, New York, 2004.

[2] K. Konopka, M. Szafran, Journal of Materials Processing Technology 175 (2006) 266–270.
[3] J.G. Miranda Hernández, S. Moreno Guerrero, A.B. Soto Guzmán, E. Rocha Rangel, Journal of Ceramic Processing Research 7 (2006) 311–315.
[4] M.I. Lieberthal, K. Kaplan, Materials Science and Engineering A 302 (2001) 83–87.
[5] H. Arik, Materials and Design 25 (2004) 31–40.
[6] S.J. Ko, K.H. Min, Y.D. Kim, I.-H. Moon, Journal of Ceramic Processing Research 3 (2002) 192–194.
[7] S. Liang, Z. Fan, L. Xu, L. Fang, Composites Part A 35 (2004) 1441–1446.
[8] S.S. Razavi Tousi, R. Yazdani Rad, E. Salahi, I. Mobasherpour, M. Razavi, Powder Technology 192 (2009) 346–351.
[9] S.M. Zebarjad, S.A. Sajjadi, Materials and Design 27 (2006) 684–688.
[10] K.H. Chung, J. He, D.H. Shin, J.M. Schoenung, Materials Science and Engineering A 356 (2003) 23–31.
[11] N. Zhao, P. Nash, X. Yang, Journal of Materials Processing Technology 170 (2005) 586–592.
[12] F. Tang, M. Hagiwara, J.M. Schoenung, Scripta Materialia 53 (2005) 619–624.
[13] F. Tang, M. Hagiwara, J.M. Schoenung, Materials Science and Engineering A 407 (2005) 306–314.
[14] M.F. Zawrah, Hamdia A. Zayed, Raghieba A. Essawy, Amira H. Nassar, Mohammed A. Taha, Preparation by mechanical alloying, characterization and sintering of Cu-20 wt% Al_2O_3 nanocomposites, Materials and Design 46 (2013) 485–490.
[15] C. Suryanarayana, Mechanical alloying and millng, Progress in Material Science 46 (2001) 1–184.
[16] T.S.S. Razavi, R. Yazdani, E. Salahi, I. Mobasherpour, Powder Technology 320 (2009) 591–602.
[17] A. Sawaby, M.S. Selim, S.Y. Marzouk, M.A. Mostafa, A. Hosny, Physica B 405 (2010) 3412–3420.
[18] P. Scherrer, Bestimmung der Grosse und der inneren Struktur von Kolloidteilchen mittels Rntgenstrahlen. Nachrichten von der Gesellschaft der Wissenschaften zu Gttingen, Mathematisch-Physikalische Klasse 2 (1918) 98.
[19] M.F. Zawrah, H. Abdel-kader, N.E. Elbaly, Materials Research Bulletin 47 (2012) 655–661.
[20] S. Sivasankarana, K. Sivaprasadb, R. Narayanasamya, P.V. Narayanasamya, Materials Characterization 62 (2011) 661–672.
[21] ASTM E384-99. Standard Test Method for Microindentation Hardness of Materials, 2005.
[22] ASTM 1327-03 Standard Test Method for Vickers Indentation Hardness of Advanced Ceramics, 2005.
[23] ASTM C1326-03. Standard Test Method for Knoop Indentation Hardness of Advanced Ceramics, 2005.
[24] A.G. Evans, E.A. Charles, Journal of the American Ceramic Society 59 (1976) 371–372.
[25] E.R. Rangel, E.R. Garcia, J.G.M. Hernández, E.T. Rojas, Journal of Ceramic Processing Research 10 (6) (2009) 744–747.
[26] H.E. Swanson, E. Tatge, National Bureau of Standard (US) Circular 539 , vol. 1, 1953, 359.
[27] R.S. Liu, et al., Modern Physics Letters 11 (1997) 1169.
[28] R. Viseslava, B. Dusan, T.J. Milan, Journal of Alloys and Compounds 459 (2008) 177–184.
[29] B. Lonnberg, Journal of Materials Science 29 (1994) 3224–3230.
[30] S.S. Razavi Tousi, R. Yazdani Rad, E. Salahi, I. Mobasherpour, M. Razavi, Powder Technology 192 (2009) 346–351.
[31] Y.D. Kim, S.T. Oh, K.H. Min, H. Jeon, I.H. Moon, Scripta Materialia 44 (2001) 293–297.
[32] J.S. Benjamin, T.E. Volin, Metallurgical and MaterialsTransactions 5 (1974) 1929.
[33] F. Zhou, J. Lee, E.J. Lavernia, Scripta Materialia 44 (2001) 2013–2017.
[34] K.H. Min, S.T. Oh, Y.D. Kima, I.H. Moon, Journal of Alloys and Compounds 352 (2003) 163–167.
[35] C.S. Torres, L. Schaeffer, Materials Research 13 (3) (2010) 293–298.
[36] F. Shehata, A. Fathy, M. Abdelhameed, S.F. Moustafa, Materials and Design 30 (2009) 2756–2762.
[37] N.C. Kothari, Dispersion Hardening by Powder Metallurgy (1984) 102.
[38] G.S. Hanumanth, G.A. Irons, Journal of Materials Science 28 (1993) 2459–2465.
[39] X. Xuan, L.S. qiang, H.U. Ping, H.M. gang, M.W. Fu, Transactions of Nonferrous Metals Society of China 19 (2009) 545–551.
[40] S. Jiao, M.L. Jenkins, R.W. Davidge, Acta Metallurgica 45 (1997) 149–156.
[41] J.G. Miranda-Hernández, S. Moreno-Guerrero, A.B. Soto-Guzmána, E. Rocha-Range, Journal of Ceramic Processing Research 7 (4) (2006) 311–314.